Gas Processing Journal

Vol. 9, No. 2 2021, pp. 1-14
http://gpj.ui.ac.ir

Research Paper

Thermodynamic evaluation and optimization of a cogeneration energy system integrated with steam network

Hamed Amiri [1], Majid Amidpour[2*], Amir Farhang Sotoodeh[3], Alireza Haji Molla Ali Kani[1]

[1] Department of Energy Engineering, Faculty of Natural Resource and Environment, Science and Research Branch, Islamic Azad University, Tehran, Iran
[2] bDepartment of Energy Systems Engineering, Faculty of Mechanical Engineering, K. N. Toosi University of Technology, No. 15, Pardis St., Molasadra Ave., Vanak Sq., Tehran, Iran
[3] Energy and Environment Faculty, Niroo Research Institute (NRI), Tehran, Iran

Received: 2020-12-12 Revised: 2021-02-08 Accepted: 2021-02-27

Abstract: Cogeneration energy systems are one of the most promising clean, efficient technologies for satisfying industrial energy needs. In this study, a cogeneration system consisting of a solid oxide fuel cell, a gasification unit, a gas turbine cycle, and a steam network module is proposed. This topping system is integrated with a steam network that provides steam for different utilities by recovering steam. Also, biomass –as renewable energy– is used to address the problems of fossil fuels, such as scarcity of resources and environmental issues. The system is evaluated from an energy perspective to ascertain the feasibility of the system. Based on the results, the efficiency attained from this system is 54.35%. An optimization study based on a genetic algorithm is performed to find the best conditions, which indicates an efficiency improvement to 65.06%. Moreover, a parametric study on different steam network pressure levels is taken place, which shows the importance of the VHP header on system performance.

keywords: Cogeneration; Steam network; SOFC; Biomass; Gasification; Gas turbine

Nomenclature

Symbols		Greek Symbols	
A	Area (cm^2)	η	Efficiency (%)
AFR	Air/fuel ratio	λ	Fuel/air ratio
BFW	Boiler feedwater		
BG	Biomass gasifier		
c_p	Specific heat at constant pressure ($kJ.kg^{-1}.K^{-1}$)	**Subscripts and superscripts**	
CC	Combustion chamber	a	Anode
CR	Compressor ratio	act	Activation
F	Faraday constant	actu	Actual
g	Gibbs energy	ADP	Acid dew point
GT	Gas turbine	BFW	Boiler feedwater

* **Corresponding Author.**
Authors' Email Address: [1] **H. Amiri** (amirihamed59@yahoo.com), [2] **M. Amidpour** (amidpour@kntu.ac.ir), [3] **A. F. Sotoodeh** (asotoodeh@nri.ac.ir), [4] **A.R Haji Molla Ali Kani** (ashkanisrbiau@gmail.com)

http://dx.doi.org/10.22108/gpj.2021.126419.1096

h	Specific enthalpy per mass ($kJ.kg^{-1}$)	c	Cathode
$\bar{h}$	Specific enthalpy per mole ($kJ.kmol^{-1}$)	comp	Compressor
HP	High pressure	cog	Cogeneration
HRSG	Heat recovery steam generator	con	Concentration
i	Current density ($A.cm^{-2}$)	c.v.	Control volume
k	Specific heat ratio	DB	Duct burner
K_p	Equilibrium constant	en	Energy
LHV	Lower heating value	f	Formation
LP	Low pressure	FG	Flue gases
M	Molar mass ($kg.kmol^{-1}$)	GM	Gas mixture
MP	Medium pressure	GT	Gas turbine
MSR	Methane steam reforming		
$\dot{m}$	Mass flow rate ($kg.s^{-1}$)	HP	High pressure
$\dot{N}$	Molar rate ($kmol.s^{-1}$)	HRSG	Heat recovery steam generator
N	Number of cells	in	Inlet
P	Pressure (kPa)	is	Isentropic
PSD	Pine sawdust	i	i^{th} component
$\dot{Q}$	Heat transfer rate (MW)	max	Maximum
$\bar{R}$	Universal gases constant ($J.kg^{-1}.K^{-1}$)	mix	Mixture
R_{Cog}	Net power/heating ratio	MP	Medium pressure
s	Specific entropy ($kJ.kg^{-1}.K^{-1}$)	N	Nernst voltage
SFR	Steam/fuel ratio	net	Net value
SN	Steam network	NG	Natural gas
SOFC	Solid oxide fuel cell	out	Outlet
ST	Steam turbine	ph	Physical
T	Temperature (K)	pp	Pinch point
U_f	Fuel utilization factor	pu	Pump
V	Voltage (V)	q	Heat transfer
VHP	Very high pressure	Rel	Relative
$\dot{W}$	Electricity (MW)	S	Supply
WSR	Water shift reaction	SOFC	Solid oxide fuel cell
		ST	Steam turbine
		Stoi	Stoichiometric
		T	Target
		top	Topping cycle
		VHP	Very high pressure

Introduction

Today, energy demand is growing at a considerable rate worldwide. Conventionally, fossil fuels have been the primary source for meeting this ever-growing demand (Ghazizadeh, Ghorbani, Shirmohammadi, Mehrpooya, & Hamedi, 2018). As a result of these fuels' utilization, the enormous volume of greenhouse gases is considered to be amongst the most dangerous threats to the environment (Bahram Ghorbani, Roshani, Mehrpooya, Shirmohammadi, & Razmjoo, 2020; Hamedi, Shirmohammadi, Ghorbani, & Sheikhi, 2015; SHEIKHI, GHORBANI, SHIRMOHAMMADI, & HAMEDI, 2014). The data published in World Energy Outlook, 2019 (Mohn & Policy, 2020), greenhouse gas (GHG) is mostly released by the power sector, which solely releases over 40 percent of energy-related carbon dioxide (CO_2) emissions. In particular, 30% of the CO_2 emission related to the energy sector is released by power plants burning coal. Therefore, a tremendous amount of effort is put by energy researchers into an efficient and clean energy system that is based on renewable energy and reduces the production of CO_2 emissions.

Solar, wind, hydro, biomass and bio-energy, geothermal, and other renewable energy resources can be utilized for a clean and sustainable generation of electricity (Ebadollahi et al., 2020; B Ghorbani, Shirmohammadi, Mehrpooya, & Assessments, 2020; Kolahi, Nemati, & Yari, 2018; Ranjbar, Nemati, & Kolahi, 2018). Because of the belief that biomass is carbon-neutral fuel, it is one of

the most favorable alternatives to fossil fuels (Gustavsson & Svenningsson, 1996). Because of the everlasting nature of replanting, biomass is considered to be a renewable energy source. In recent years, the biomass gasification process has seen several advancements, and now it can be used to convert solid biomass to gaseous fuels utilized for power generation (Ebrahimi, Ghorbani, & Ziabasharhagh, 2020; Ebrahimi, Ghorbani, Ziabasharhagh, & Rahimi, 2020). Generally, there are two methods for consuming biomass energy: Combustion and Gasification. In combustion, a combustor is used to combust solid biomass, and the heat in the combustion products is utilized for operating power cycles, organic Rankine cycle (ORC), and gas turbine (GT) cycle, etc. Gasification is the second method, which through it the solid biomass convert into syngas, a combustible gas mixture. Hydrogen (H_2), carbon monoxide (CO), methane (CH_4), water vapor (H_2O), carbon dioxide (CO_2), and nitrogen (N_2) are among the main components of syngas (Hu et al., 2016). Afterward, this syngas, also called producer gas, is used in different power systems as fuel. The gasification method is believed to be much more efficient than the combustion process (Niasar, Ghorbani, Amidpour, & Hayati, 2019; Shariati Niasar et al., 2017). Because of the advantages of biomass-fueled cogeneration energy systems, today, these systems are considered one of the most prominent options for meeting the demands of power and heating/cooling in an efficient and environmentally friendly manner. One of the essential advantages of cogeneration is power, heating or cooling, from a solo source simultaneously (Pirmohamadi, Ghaebi, Ziapour, & Ebadollahi, 2021; Rostamzadeh, Ebadollahi, Ghaebi, Shokri, & management, 2019). The heating can be achieved by utilizing waste energy from the prime mover exit which can be used in hot water and steam production and also space heating.

Fuel cells have advantages that have made favorable options for power generating. In addition to high efficiency, the fuel's chemical energy directly converses to power without any necessary combustion. High-temperature fuel cells are the most favorable option for designing biomass gasification-based energy systems (Radenahmad et al., 2020) due to the similarity of the high-performance cell's operational temperature to the biomass gasification process (Archer & Steinberger-Wilckens, 2018). Among this type of fuel cells, solid oxide fuel cell (SOFC) is a high potential (Tafazoli, Shakeri, Baniassadi, & Babaei, 2017) and an appropriate option that can be efficiently integrated with a gas turbine (GT), steam turbine (ST), organic Rankine cycle (ORC), Kalin Cycle (KC), Stirling engine, supercritical CO_2 (s-CO_2) cycle, and other energy conversion technologies. Besides, SOFC yields byproducts like heat, which can be utilized by cogeneration facilities.

SOFC/GT systems have been studied by researchers in several papers that have analyzed the performance of these systems considering different fuels, temperature levels, and arrangements. For example, Cheddie et al. (Cheddie, 2011) integrated SOFC and a gas turbine power plant capable of 10 MW power generation in an indirect manner that resulted in 4.65 ¢/kWh per—unit of energy cost. They also carried out the same analysis using semi-direct coupling and anode recycling (Cheddie & Murray, 2010). In 2008, Akkaya et al. (Akkaya, Sahin, & Huseyin Erdem, 2008) conducted a thermodynamical simulation of SOFC and CHP turbines under stable conditions. In another study, Akkaya and Sahin (Akkaya & Sahin, 2009) devised a steady-state mathematics model of integrating solid-state oxide fuel and organic Rankine cycle (ORC). In 2014, Calindro et al. (Caliandro, Tock, Ensinas, & Marechal, 2014) analyzed a SOFC/GT system from a multi-objective thermal economy perspective. Improving electricity efficiency and minimizing investment costs were among the objectives of this research. According to the results, the SOFC/GT system's power generation efficiency is up to 50%, which is high, but the SOFC/GT system still has a high exhaust temperature. Significant progress has been made in the thermal efficiency and economy of SOFC/GT systems, but still, the exhaust gas from SOFC/GT is not utilized appropriately. Using this exhaust gas, a waste heat recovery cycle helps to improve system efficiency. The system's total energy conversion efficiency can be improved by recovering the SOFC/GT waste heat (Larminie & Dicks, 2000; Meng et al., 2017). In another study, Ghorbani and Khoshgoftar Manesh analyzed an IRSOFC-GT-ORC Hybrid System from the thermodynamic, exergetic, exergoeconomic, and advanced energetic points of view. The results showed that net power and overall cycle efficiency increased by 1.1 MW and 7.7% compared to the basic SOFC-GT comparison. Exergy efficiency also was increased by 3.6 % rather than the initial base case (S. Ghorbani & Khoshgoftar Manesh, 2020).

There are two primary purposes for using waste heat in power plants: heating liquid water and heating coal in gas units. Reducing this heat results in increasing efficiency and reducing emissions (Iglesias Garcia, Ferreiro Garcia, Carbia Carril, & Iglesias Garcia, 2018; Moradi et al., 2019). Many researchers have been done about reducing the heat dissipated in different units of an energy system in recent years. This waste heat can be a result of combustion in the GT (Kadhum, 2016). It also can be a result of reducing heat produced in combustion engines. The waste heat is recognized as low-grade waste heat, and its reduction can lead to a decrease in environmental pollution and lower carbon dioxide and similar gasses release. Reducing fuel consumption can also result in a decrease in the emission rate of pollutants. The utility part is one of the crucial parts of any process system. The generation of power is necessitated for the process, and steam production occurs at different levels of the process (Arghandeh, Amidpour, & Khodaei, 2009).

The optimization of the solar heat and power (CHP) system has become the subject of further research in recent years (Bahram Ghorbani et al., 2019). For example, the Cuckoo Search algorithm is utilized for optimizing decision variables (M. H. Khoshgoftar Manesh & Ameryan, 2016). As a matter of fact, fuel consumption reduction results in

decreasing both costs and environmental emissions. A steam grid is used to produce the power and steam necessitated for the process. Steam efficiency will have effects on the efficiency of the whole process. Also, an accurate site utility design can lead to a reduction in investment costs and also saving more energy. For example, Khoshgoftar Manesh and Noori Shemirani (Mohammad Hasan Khoshgoftar Manesh & Noori Shemirani, 2017) simulated and optimized utilities in an oil refinery concerning exergetic, exergoeconomic, and environmental analyses. According to their study results, the annual cost was declined to 42% in the best scenario.

Several studies have been made about reducing low-temperature waste in units previously mentioned (Wang, Wang, & Zhang, 2012). The amount of waste heat dissipated from industrial units reduces, resulting in saving energy and preventing further environmental pollution (Varbanov, Doyle, & Smith, 2004). Zheng et al. (Zheng et al., 2017) conducted a feasibility study on a low-grade heat recovery cycle in the petrochemical industry. According to statistics, low-temperature heating comprises 50% of heat dissipation from each industrial sector (Jouhara et al., 2018). Using the Rankine cycle for recovering waste heat in various industrial sectors is one of the first solutions that can be proposed. However, it is not economically feasible to recover low-temperature waste using a Rankine cycle (Johnson & Choate, 2008).

According to the given literature review, the integration of renewable resources with industrial steam networks has not been thoroughly investigated. Thus, In this study, a biomass-based cogeneration scheme integrated with a steam network is assessed and evaluated from the thermodynamic viewpoint, and afterward, an optimization study is performed to find the optimum design conditions.

2. Systems description

In Fig. 1, the layout of the proposed integrated cogeneration system is depicted. According to this figure, the devised set-up encompasses these components: a BG, a SOFC module, a GT cycle, and an SN. The following describes each unit:

In BG, biomass is fed into the gasifier at ambient condition (state 5). A compressor is used to boost the low-pressure steam extracted from the SN to the necessitated high-pressure steam. Simultaneously, a fragment of the compressed air (state 3) is led into the gasifier also. After the syngas is generated (state 6), which is a result of gasification processes in the gasifier, it splits into two streams: the first stream is guided into the combustion chamber (CC) of the GT cycle (state 8), at the same time as the second one is injected into SOFC (state 7).

In the SOFC module, a recuperator is utilized for preheating the rest of the compressed air at state 4. Afterward, this preheated air is guided into the cathode part of the SOFC module (state 9). Simultaneously, the syngas generated in the gasifier is directed to the anode part of the module and then being utilized in the methane reforming process for producing CO and enriching H_2. A reaction occurs between CO and steam during the water shifting process, and then it transforms into CO_2. It is worthy to note that through moving from cathode to anode, ions of O_2 are combined with H_2, which results in the generation of steam. Meantime, electricity is generated through the movement of electrons from the anode toward the cathode. A percentage of the released heat during the electrochemical reaction is utilized to satisfy the direct internal reforming process's thermal demands. The rest of the heat mentioned earlier is used to warms up the residual reactants and the FC (fuel cell) products. When the electrochemical reaction comes to an end, the unreacted syngas and the surplus air are released from the anode and cathode compartments, respectively. Afterward, these two released gases enter the combustion chamber. The flue gas exiting from the combustion chamber (state 12) is utilized to preheat the air stream and then is guided into the gas turbine (state 13).

In the GT cycle, an air compressor (AC) is used to compress the air at ambient pressure (state 1). Afterward, the produced compressed air splits into two flows: The first one is guided into the aforementioned preheating process using a recuperator and then goes into the SOFC module, while the second flow part is guided into the gasifier. For providing shaft power of the AC, the flue gases at the recuperator's outlet (state 12) are expanded through a gas turbine. Also, surplus power for direct users is generated by this expansion. At the final step, while their temperature has been decreased, the flue gases leave the gas turbine and then are guided into a heat recovery steam generator (HRSG). In the HRSG, steam necessitated for gasification and heating loads for wide-site utility sectors are generated simultaneously.

Auxiliary fuel is necessary to provide a surplus amount of load that the HRSG unit needs for heating and steam generation purposes. In the integration of SN/HRSG, NG is utilized as this necessary auxiliary fuel. There are four stages in the process of power and heating generation along with steam supplement: very high pressure (VHP), high pressure (HP), medium pressure (MP), and low pressure (LP). To achieve this goal, three steam turbines (STs) are utilized at each stage in which the expansion process for power generation takes place in STs. To adjust the mass flow rate of steam exchanged between successive stages, an expansion device is used, which is also known as a letdown process. After the necessitated steam for each utility center is extracted at each stage, a fraction of residue is bypassed for the gasification process's steam supply.

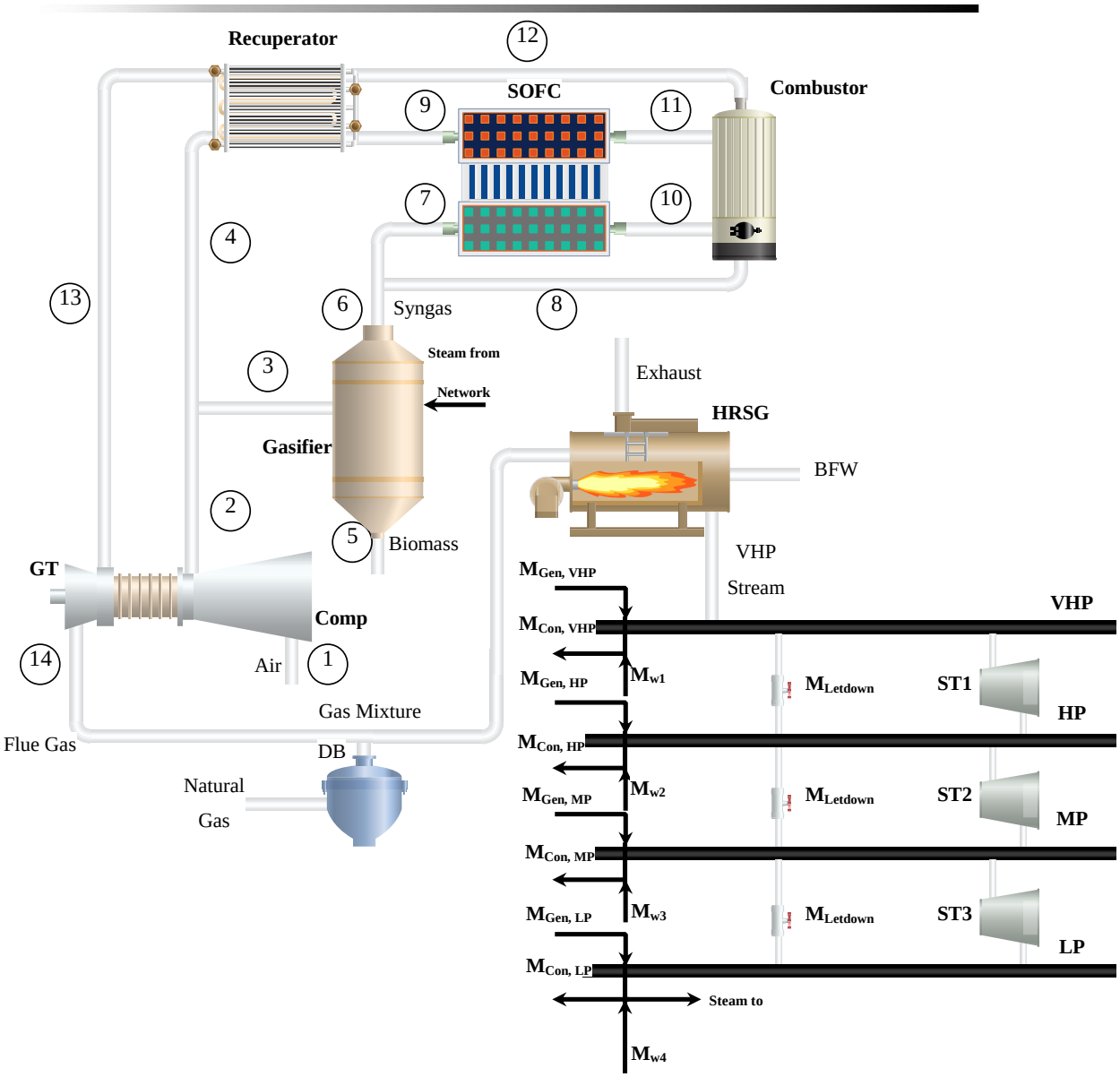

Figure 1: Schematic of the proposed biomass-based cogeneration system.

Methodology

Before developing the thermodynamic models, some assumption is necessary to be made. The following represent general assumptions (Bezaatpour, Rostamzadeh, Bezaatpour, & Ebadollahi, 2021; Ghaffarpour, Mahmoudi, Mosaffa, & Farshi, 2018; Ghaffarpour, Mahmoudi, Mosaffa, Farshi, & management, 2018; Smith, 2005; Sun, Doyle, & Smith, 2015; Sun, Smith, & Research, 2015; M. Taheri, A. Mosaffa, & L. G. J. E. Farshi, 2017):

- The system is operating in a steady-state.
- The air consists of 79% and 21% of N_2 and O_2, respectively.
- Heat losses between all the heat exchangers, pipelines, and the environment are not taken into account.
- In the SOFC, the pressure at the anode and the cathode is assumed to be constant and equal. Similarly, the pressure drop of the heat exchanger remains constant.
- All the reactions reach chemical equilibrium before leaving the SOFC.
- Fuel and air are assumed to be ideal gas.
- The only electrochemically active species is hydrogen.
- Potential and kinetic energy effects are assumed to be negligible.
- Isentropic efficiency of the GT and AC is assumed to be 80% and 75%, respectively. For all steam turbines, a variable isentropic efficiency related to input load is assumed.
- The desuperheating process of the Superheated steam in the deaerator uses water.
- The acid dew point of the flue gases leaving the GT is 120℃.
- The pressure of deaerators is set on 1.02 bar, and its temperature is saturated liquid at this pressure.
- For steam recovery, all processes taking place in the SN unit use desuperheater steam. The temperature of all elements in the SN is set below 570℃.

• The steam generation process uses boiler feed water (BFW) at the deaeration temperature.

Energy analysis

To evaluate the devised system's performance, each element is considered a control volume and mass and energy balance equations to be employed for them individually (Bahram Ghorbani, Hamedi, & Amidpour, 2016). The general form of mass and energy balance equations at steady state for inlet and outlet streams of a control volume with heat transfer and work interactions can be articulated as follows:

$$\sum \dot{m}_{in} - \sum \dot{m}_{out} = 0 \quad (1)$$

$$\sum (\dot{m}h)_{in} - \sum (\dot{m}h)_{out} + \sum \dot{Q}_{in} - \sum \dot{Q}_{out} + \dot{W} = 0 \quad (2)$$

Biomass gasification

Pine sawdust (PSD) is selected as biomass for the devised system (Altafini, Wander, & Barreto, 2003; Ghaffarpour, Mahmoudi, Mosaffa, & Farshi, 2018). The critical characteristics of PSD are listed in Table 1. The following relation can be used for computing compressed air temperature (T_2) (Ghaffarpour, Mahmoudi, Mosaffa, & Farshi, 2018; M. Taheri, A. Mosaffa, & L. G. Farshi, 2017):

$$\frac{T_2}{T_1} = 1 + \frac{1}{\eta_{is,comp}}\left((CR)^{\frac{k-1}{k}} - 1\right) \quad (3)$$

In this relation, CR represents the compressor ratio (P_2/P_1), T_1 shows the air temperature at ambient condition, k is the specific heat ratio, and $\eta_{is,comp}$ represents the isentropic efficiency of the compressor, which is computed by the following relation:

$$\eta_{is,comp} = \frac{h_1 - h_{2,is}}{h_1 - h_2} \quad (4)$$

Table 1: Biomass feedstock characteristics (Altafini et al., 2003)

Biomass type	Pine sawdust
LHV (kJ kg^{-1})	23716.54
Carbon (%)	52.28
Hydrogen (%)	5.20
Oxygen (%)	40.85
Nitrogen (%)	0.47

The following reaction shows the chemical reaction in the gasifier, which takes place due to the supply of biomass and high-temperature steam and air (Ghaffarpour, Mahmoudi, Mosaffa, & Farshi, 2018):

$$(C_{a_1}H_{a_2}O_{a_3}N_{a_4})_{Ash\ free\ dry\ fuel} + (a_5(O_2 + 3.76N_2))_{air} + (a_6H_2O_{gas})_{steam} \Rightarrow (b_1CH_4 + b_2CO + b_3CO_2 + b_4H_2 + b_5H_2O + b_6N_2)_{Syngas} \quad (5)$$

the coefficient a_1 is equal to 1 for every single atom of carbon in biomass fuel. To compute the coefficients a_2, a_3, and a_4, mole ratios should be used as follows:

$$a_2 = \frac{(X_H/M_H)}{(X_C/M_C)}, \quad a_3 = \frac{(X_O/M_O)}{(X_C/M_C)}, \quad a_4 = \frac{(X_N/M_N)}{(X_C/M_C)} \quad (6)$$

$$M_{dry\ fuel} = a_1M_C + a_2M_H + a_3M_O + a_4M_N \quad (7)$$

The definition of stoichiometric air-fuel ratio (AFR_{Stoi}) is shown in Eq. (8). Also, the relative air-fuel ratio (AFR_{Rel}) and AFR_{Stoi} can be used to determine the actual air-fuel ratio (AFR_{act}) as shown in Eq. (9) (Ghaffarpour, Mahmoudi, Mosaffa, & Farshi, 2018; Srinivas, Gupta, & Reddy, 2009):

$$AFR_{Stoi} = (a_1 + 0.25a_2 - 0.5a_3)M_{air} \quad (8)$$

$$AFR_{Act} = AFR_{Rel} \times AFR_{stoi} \quad (9)$$

In these relations, AFR_{Rel} is equal to 0.1.

The coefficients a_5 and a_6 can be calculated by the following relations, respectively (Ghaffarpour, Mahmoudi, Mosaffa, & Farshi, 2018):

$$a_5 = \frac{AFR_{Act} \times M_{dry\ fuel}}{M_{air}} \quad (10)$$

$$a_6 = \frac{SFR \times M_{dry\ fuel}}{M_{H_2O}} \quad (11)$$

In Eq. (11), SFR represents the steam-fuel ratio. Considering atom balances on carbon, hydrogen, oxygen, and nitrogen, the following relations can be written about coefficients $a_{1\text{-}4}$:

$$Carbon\ balance: \quad a_1 = b_1 + b_2 + b_3 \quad (12)$$

$$Hydrogen\ balance: \quad a_2 + 2a_6 = 4b_1 + 2b_4 + 2b_5 \quad (13)$$

$$Oxygen\ balance: \quad a_3 + 2a_5 + a_6 = b_2 + 2b_3 + b_5 \quad (14)$$

$$Nitrogen\ balance: \quad a_4 + 2 \times 3.76a_5 = 2b_6 \quad (15)$$

To obtain the composition of the produced syngas, there are six unknown and four equations. Therefore, in order to compute the unknowns, two more equations are necessitated. These equations are developed from equilibrium reactions, as follows:

$$Methane\ steam\ reforming: \quad CH_4 + H_2O = CO + 3H_2 \quad (16)$$

$$Water\ shift\ reaction: \quad CO + H_2O = CO_2 + H_2 \quad (17)$$

Because of the stable methane molecule, the methane steam reforming reaction has an endothermic nature. A high process temperature is needed to shift the dissociation reaction's equilibrium composition to the right side. On the contrary, the water gas shift reaction is exothermic, and therefore to shift the equilibrium to the right side, the process temperature should be as low as possible. Eqs (12-15) can be rewritten in terms of two unknown coefficients, i.e., b_1 and b_2:

$$b_3 = a_1 - b_1 - b_2 \quad (18)$$

$$b_4 = 2a_1 + 0.5a_2 - a_3 - 2a_5 - 4b_1 - b_2 \quad (19)$$

$$b_5 = a_3 + 2a_5 + a_6 - 2a_1 + 2b_1 + b_2 \quad (20)$$

$$b_6 = 0.5a_4 + 3.76a_5 \quad (21)$$

The following relation can be used to compute the total number of species in products:

$$n_t = b_1 + b_2 + b_3 + b_4 + b_5 + b_6 = a_1 + 0.5a_2 + 0.5a_4 + 3.76a_5 + a_6 - 2b_1 \quad (22)$$

In Eqs (23) and (24), are the equilibrium constants of the reforming reaction (K_{p,R_G}) and water shift reaction (K_{p,WS_G}) are computed:

$$K_{p,R_G} = \frac{P_{CO}P_{H_2}^3}{P_{CH_4}P_{H2O}} = \frac{b_2 b_4^3 (\frac{P_{gasifier}}{P_0})^2}{b_1 b_5 n_t^2} \quad (23)$$

$$K_{p,WS_G} = \frac{P_{CO_2}P_{H_2}}{P_{CO}P_{H_2O}} = \frac{b_3 b_4}{b_2 b_5} \quad (24)$$

The following relation shows the equilibrium constant based on Gibbs energy:

$$\ln K_P = \frac{-\overline{\Delta G}^0}{\bar{R}T_{gasifier}} \quad (25)$$

In this relation, $\overline{\Delta G}^0$ represents the Gibbs free energy for each reaction and can be calculated as follows:

$$\overline{\Delta G}^0 = \sum \bar{h}_f^0 + \left(\bar{h}_{T_{gasifier}} - \bar{h}_{T_0}\right) - T_{gasifier}\bar{S}_{T_{gasifier}} \quad (26)$$

Solid oxide fuel cell (SOFC)

Mass and energy balance equations are used to develop the thermodynamic modeling framework (C. Ozgur Colpan, Hamdullahpur, Dincer, & Yoo, 2010; Ghaffarpour, Mahmoudi, Mosaffa, Farshi, et al., 2018; Guo, Yu, Li, & Zhao, 2020). Considering the above assumptions, the following three reactions occur in the SOFC:

Reforming: $CH_4 + H_2O \rightarrow CO + 3H_2$ (27)

Shift: $CO + H_2O \rightarrow CO_2 + H_2$ (28)

Electrochemistry: $H_2 + \frac{1}{2}O_2 \rightarrow H_2O$ (29)

It is assumed that the reforming reaction is fully developed, and therefore, the methane is wholly converted in the process. This reaction's full development is because of the high temperature of the reactor and the catalyst effect. It is assumed that the shifting reaction is considered to will reach a thermodynamic equilibrium state. the equilibrium constant in this state can be given by:

$$K_{ps} = \frac{X_{CO_2}X_{H_2}}{X_{CO}X_{H_2O}} \quad (30)$$

$$\log K_{ps} = AT^4 + BT^3 + CT^2 + DT + E \quad (31)$$

In Eq. 31, A, B, C, D, and E represent the constant values (See Table 2), and T is the fuel cell's operating temperature.

Table 2: Coefficients for equilibrium constants (Mehr, Mahmoudi, Yari, & Chitsaz, 2015)

Parameter	A	B	C	D	E
Value	5.4730×10^{-12}	-2.5747×10^{-8}	4.63742×10^{-5}	-3.915×10^{-2}	13.2097

In order to compute the output voltage V_{cell} of SOFC, the irreversible loss of each part should be subtracted from the ideal reversible voltage V_{Nernst}:

$$V_{cell} = V_{Nernest} - V_{ohm} - V_{act} - V_{conc} \quad (32)$$

In this relation, V_{cell} and V_{Nernst}, represent the actual output voltage and the ideal reversible voltage, respectively. V_{act}, V_{conc}, and V_{ohm} are the activated polarization overvoltage, the concentration polarization overvoltage, and the ohmic polarization overvoltage. The reversible ideal voltage V_{Nernst} is defined as the voltage without current passing through the SOFC external circuit. The following relation expresses the V_{Nernst}:

$$V_{Nernest} = E_0 - \frac{RT_{PEN}}{2F} \times \ln\left(\frac{x_{H_2}\sqrt{X_{o_2}}}{x_{H_2O}}\right) \quad (33)$$

Butler-Volmer equation is used for computing the activated polarization overvoltage:

$$V_{act} = \frac{2RT}{n_eF} sinh^{-1}(\frac{i}{2i_0}) \quad (34)$$

In this relation, n_e represents the number of exchanged electrons.

The concentration polarization overvoltage is expressed in the following relations:

$$V_{conc} = -\frac{RT}{n_eF}\ln\left(1 - \frac{i}{i_{as}}\right) + \frac{RT}{n_eF}\ln\left(1 + \frac{\mathcal{P}_9^{H_2}}{\mathcal{P}_9^{H_2O}}\frac{i}{i_{as}}\right) - \frac{RT}{2n_eF}\ln\left(1 - \frac{i}{i_{cs}}\right) \quad (35)$$

where i_{as} and i_{cs} represent the anodic and cathodic limiting current density, respectively.

Ohm's law is used in the following relation to calculate ohmic polarization overvoltage:

$$V_{ohm} = \mathrm{i}\sum_k \delta_k A_k exp\ (\frac{B_k}{T}) \quad (36)$$

Eq. 37 is used for calculating the electrochemical reaction rate in Eq. (37):

$$r_{H_2} = \frac{JA_R}{2F} \quad (37)$$

In this relation, r_{H2} represents the H_2 electrochemical reaction rate. A, J, E_A, and F represent effective reaction area, the current density, activation energy, and Faraday constant, respectively. The steam-to-carbon ratio (STCR) of the anode stream is expressed as:

$$STCR = \frac{(n_{H_2O})_{in}}{(n_{H_2O} + n_{CO} + n_{CO_2})_{in}} \quad (38)$$

The following relation is used to compute the SOFC fuel utilization ratio of SOFC (U_f):

$$U_f = \frac{n_{H_2}}{n_{CH_4,in} + n_{CO,in} + n_{H_2O,in}} \quad (39)$$

where n_i represents the molar flow rate of H_2, CH_4, CO, H_2O.

The power output of the SOFC stack is calculated as follows

$$W_{SOFC} = JV_{cell}NA \quad (40)$$

N, in this relation, represents the total number of cells. A represents the active area of a single fuel cell. The values and constants for electrochemical reaction calculation are shown in Table 2.

In Eq. 41, the general energy conservation equation is represented:

$$Q - W = \sum m_{out}h_{out} - \sum m_{in}h_{in} \quad (41)$$

Then In SOFC, the energy balance equation can

be written as follows:

$$\sum m_{in}h_{in} + m_{CH_4}Q_{CH_4} = \sum m_{out}h_{out} + W_{SOFC} \quad (42)$$

where W_{SOFC} represents the SOFC power output.

Combustor and gas turbine module

Since the content of CH_4 is not enough to carry on the combustion process in the combustor, some surplus amount of syngas is bypassed from the gasifier (state 8). Therefore, Eq (43) can be used to express the reaction taking place in the combustion chamber (Ghaffarpour, Mahmoudi, Mosaffa, & Farshi, 2018):

$$A_1CH_4 + A_2CO + A_3CO_2 + A_4H_2 + A_5H_2O + A_6N_2 + a_{th}O_2 \rightarrow x_1CO_2 + x_2H_2O + x_3N_2 + x_4O_2 \quad (43)$$

In this Equation, A_i represents the sum of mole rate at states 9 and 7.

At the outlet GT, the gas temperature can be computed by the following relation:

$$\frac{T_{14}}{T_{13}} = 1 - \eta_{is,GT}\left(1 - \left(\frac{P_{13}}{P_{14}}\right)^{\frac{1-k}{k}}\right) \quad (44)$$

In this relation, $\eta_{s,GT}$ represents the isentropic efficiency of gas turbine and k represents the flue gas specific heat ratio, which can be calculated as follows:

$$k_{flue\ gas} = \frac{C_{p,mix}}{C_{v,mix}} \quad (45)$$

In Table. 3, necessitated data for simulation and modeling of the proposed cogeneration system are listed.

Table 3: Some required data for simulation of the devised cogeneration system (C Ozgur Colpan, Dincer, & Hamdullahpur, 2007).

Parameters	Value
Reference temperature, $T_0\ (K)$	298.2
Reference pressure, $P_0\ (kPa)$	101.3
Biomass flow rate, $\dot{m}_{biomass}\ (kg.s^{-1})$	10
Steam to fuel ratio, $SFR\ (kmol.kmol^{-1})$	1
Air compressor pressure ratio, CR	10
SOFC outlet temperature, $T_{SOFC}\ (K)$	1023.2
SOFC outlet and inlet temperature difference, $\Delta T_{SOFC}\ (K)$	100
Active surface area of fuel cell, $A_{cell}\ (cm^2)$	100
Number of cells, N_{cell}	1000
Current density of SOFC, $i_{SOFC}\ (A.cm^{-2})$	0.3

Steam network

A fully detailed representation of steam network modeling is represented and described in our previous work (Amiri, Sotoodeh, & Amidpour, 2021). Also, the targeting algorithm implemented in this study is represented in Fig. 2.

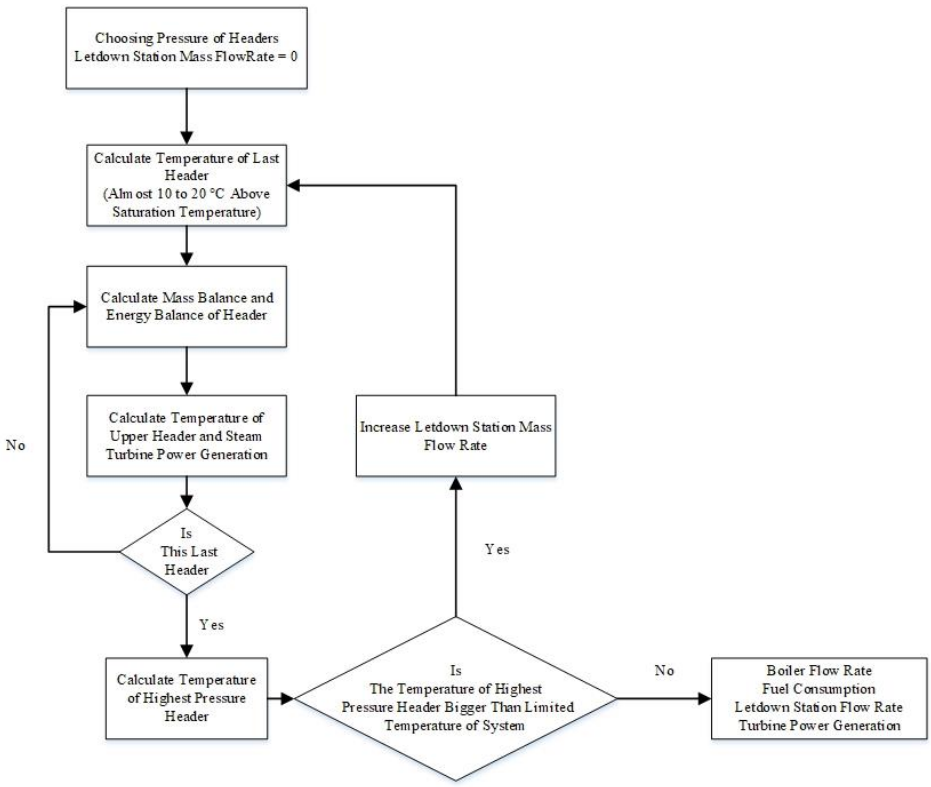

Figure 2: Targeting algorithm for the proposed system in the steam network.

Performance evaluation

The energy efficiency of the proposed system can be described as follows:

$$\eta_{en,cog} = \frac{\dot{W}_{Net,cog} + \dot{Q}_{Consumption}}{\dot{m}_{Biomass} \times LHV_{Biomass} + \dot{m}_{NG} \times NHV_{NG} + \dot{Q}_{Generation}} \quad (46)$$

where, $\dot{W}_{Net,cog}$ is the net power which is

described as follows:

$$\dot{W}_{Net,cog} = \dot{W}_{SOFC} + \dot{W}_{GT} + \dot{W}_{ST1} + \dot{W}_{ST2} + \dot{W}_{ST3} - \dot{W}_{comp} \quad (47)$$

Model Validation

In this study, Engineering Equation Solver (EES) is used to establish the performance of the proposed cogeneration system (Klein & Nellis, 2012). The current computational and experimental results in the literature are used to evaluate the validity of this model. For gasification and SOFC, the comparisons between the modeling results are represented in Table 4 and Fig. 3, which show good accuracy.

Table 4: Comparison results of gasification modeling.

Syngas composition (dry basis, mol %)	Present work	Srinivas et al. (Srinivas et al., 2009)
CH_4	2.69	0.01
CO	18.14	20.3
CO_2	10.08	9.5
H_2	18.01	19.5
N_2	51.64	50.69

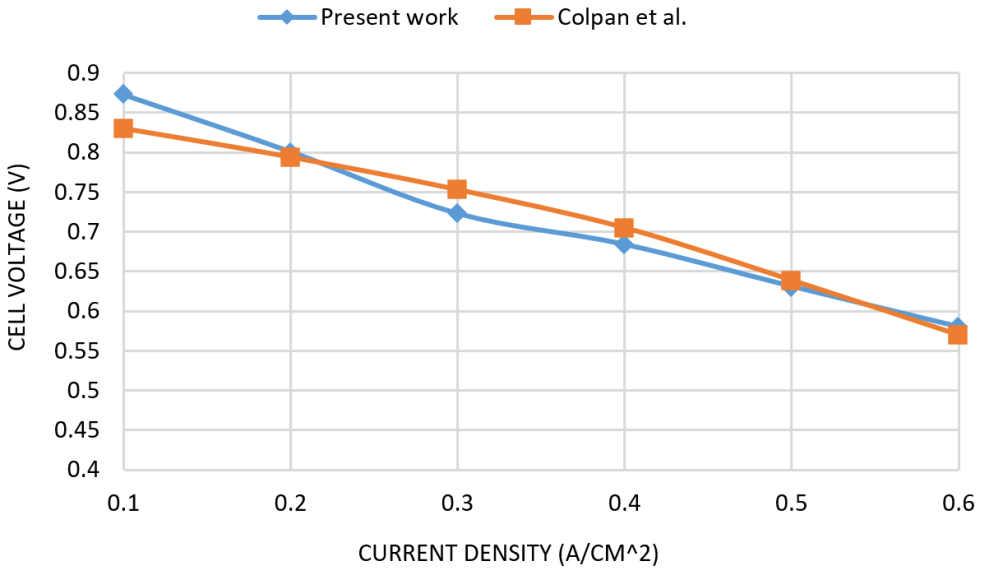

Figure 3: Comparison of SOFC modeling outcomes between the present study and Colpan et al. (C Ozgur Colpan et al., 2007).

Table 5: Verification of simulation results for the steam network (power calculation).

Pressure of header	Temperature of header (°C)			M_{Output} (kg S^{-1})		
	Sun et al. (Sun, Doyle, et al., 2015)	Present study	Error (%)	Sun et al. (Sun, Doyle, et al., 2015)	Present study	Error (%)
VHP	570	570	0	0	0	0
HP	378.6	382.3	0.98	26.4	29.81	12.92
MP	283.2	285.9	0.95	47	50.05	6.49
LP	171.8	171.9	0.06	33.9	34.39	1.44

Table 5: Verification of simulation results for the steam network (power calculation).

Pressure of header	Temperature of header (°C)			M_{Output} (kg S^{-1})		
	Sun et al. (Sun, Doyle, et al., 2015)	Present study	Error (%)	Sun et al. (Sun, Doyle, et al., 2015)	Present study	Error (%)
VHP	570	570	0	0	0	0
HP	378.6	382.3	0.98	26.4	29.81	12.92
MP	283.2	285.9	0.95	47	50.05	6.49
LP	171.8	171.9	0.06	33.9	34.39	1.44

Table 6: Verification of simulation results for the steam network (power calculation).

Steam turbine	Generated power (MW)		
	Sun et al. (Sun, Doyle, et al., 2015)	Present study	Error (%)
Steam turbine 1 (ST 1)	10.5	10.23	2.57
Steam turbine 2 (ST 2)	6.77	7.03	3.84
Steam turbine 3 (ST 3)	5.82	6.23	7.04

Finally, for evaluating the steam network, the results of simulations are compared with Sun et al. (Sun, Doyle, et al., 2015). In Tables 5 and 6, the results of this validation for mass flow rate and power are shown, respectively. As can be deduced from this comparison, a good agreement exists between the results of the two studies.

4. Result and discussion

The main results of the energy analysis of the reckoned cogeneration system are listed in Table 7. According to the results, the net electricity is augmented by approximately 52% after integrating the combined SOFC/GT system with the steam network. Besides that, 235.266 MW heating energy can be produced along with 72.3 MW amount of net power. Finally, the energy efficiency of this system is 54.35%, which shows much more performance compared to the standalone SOFC/GT scheme.

Table 7: Performance indicators of the present study.

Parameter	Value
$\dot{W}_{SOFC}$ (MW)	25.75
$\dot{W}_{GT}$ (MW)	30.56
$\dot{W}_{Comp}$ (MW)	8.76
$\dot{Q}_{Consumption}$ (MW)	235.266
$\dot{W}_{Net,top}$ (MW)	47.55
$\dot{W}_{Net,cog}$ (MW)	72.3
$\eta_{en,top}$ (%)	20.05
$\eta_{en,cog}$ (%)	54.35
R_{Cog}	0.3073

Moreover, steam network targeting results are depicted in Fig. 4.

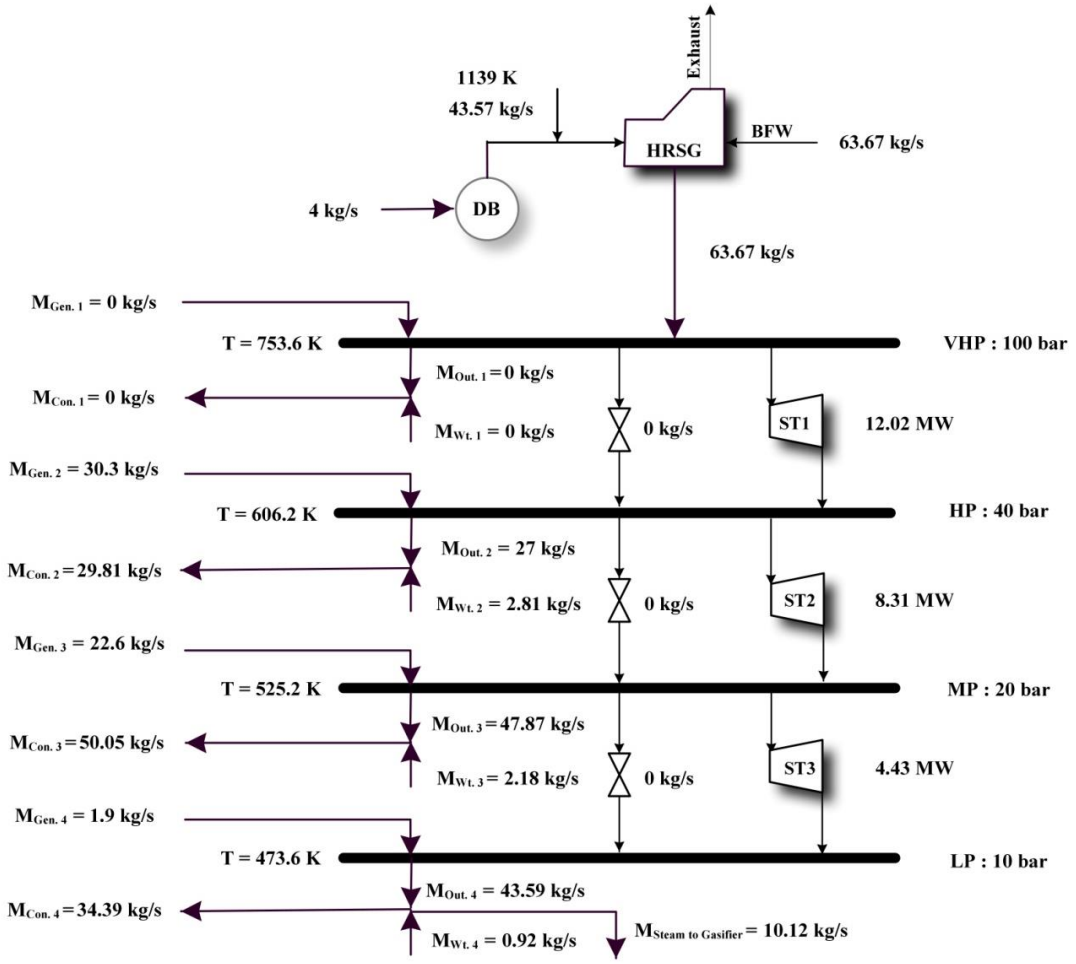

Figure 3: Results of simulation for steam network targeting for a maximum steam temperature of 570℃.

Parametric study of steam network side

A parametric study is applied to investigate the impact of pressure headers of the steam network. The variations of energy efficiency with various steam network pressure headers are depicted in Fig. 4. According to this figure, it can be deduced that with increasing *VHP*, the energy efficiency is raised since the extraction ratio of the first turbine increases remarkably. In the HP header case, the energy efficiency decreases with the increase of HP, which is due to the more significant effect of heating load decrease than the impact of power augmentation. Similarly, as pressure increases in MP headers, the power generated by steam turbines and the heating capacity decreases since expansion ratios of superior turbines decreases. As expected, VHP headers have a higher impact on efficiency since

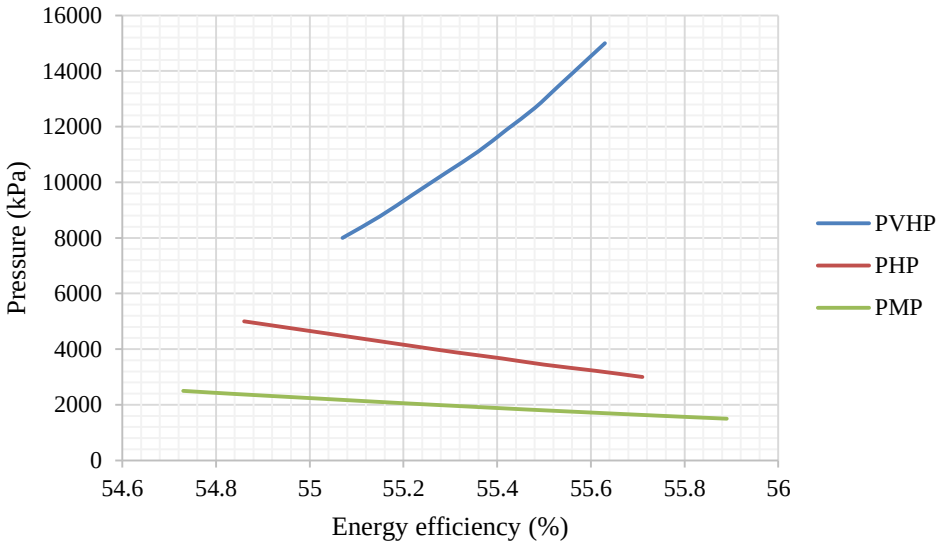

Figure 4: Impact of steam network headers on energy efficiency.

Optimization study

Genetic-based optimization has been carried out in this study. The genetic algorithm method's various parameters such as population size, number of generations mate, selection probability, and mutation rates are optimized for having the best-appropriate time and accuracy (Mohsenipour, Ahmadi, Mohammadi, Ebadollahi, & Amidpour, 2019). The main goal of this optimization is the maximization of energy efficiency by considering a single parameter as an objective function. While the number of fuel cells (N_{cell}), compression ratio (CR), steam fuel ratio (SFR), SOFC operating temperature (T_{SOFC}) are specified as the decision variables, respectively. The results of the optimization are represented in Table 8.

Table 8: Genetic algorithm parameters

Variables	Range of difference	Optimization results
Number of fuel cells (N_{cell})	800-1200	1098
Compression ratio (CR)	10-19	10
Steam fuel ratio (SFR)	0.7-1.5	1.063
SOFC operating temperature (T_{SOFC}) (K)	923-1073	955.3
Energy efficiency (%)	-	65.06

4. Conclusion

Energy efficiency represents a noteworthy part of sustainability development. Cogeneration systems are one of the promising clean-efficient technology for satisfying industrial energy needs. In this paper, a biomass CHP system integrated with a steam network has been explored. The proposed cogeneration system consists of a solid oxide fuel cell, a gasifier, a gas turbine system, and a steam network module. The required steam in the gasifier was provided by using a fraction of generated steam in the LP level of the steam network. Natural gas was exploited as an auxiliary fuel to provide the extra required fuel needed for steam generation in the steam network module. The set-up is investigated from energetic viewpoints to determine the feasibility of the system. Based on energy analysis, the efficiency obtained from this system is 54.35%. To find the optimum operating conditions of this system, an optimization study is also carried out, which suggests an efficiency improvement to 65.06% based on optimized decision variables. Also, a parametric study on different steam network pressure levels is taken place, which shows the importance of VHP levels on system performance. This new configuration could bring a new concept through the field of industrial energy integration.

References

Akkaya, A. V., & Sahin, B. (2009). A study on performance of solid oxide fuel cell-organic Rankine cycle combined system. *International Journal of Energy Research, 33*(6), 553-564. doi:10.1002/er.1490

Akkaya, A. V., Sahin, B., & Huseyin Erdem, H. (2008). An analysis of SOFC/GT CHP system based on exergetic performance criteria. *International Journal of Hydrogen Energy, 33*(10), 2566-2577. doi:10.1016/j.ijhydene.2008.03.013

Altafini, C. R., Wander, P. R., & Barreto, R. M. (2003). Prediction of the working parameters of a wood waste gasifier through an equilibrium model. *Energy conversion and management, 44*(17), 2763-2777.

Amiri, H., Sotoodeh, A. F., & Amidpour, M. (2021). A new combined heating and power system driven by biomass for total-site utility applications. *Renewable Energy, 163*, 1138-1152. doi:https://doi.org/10.1016/j.renene.2020.09.039

Archer, S. A., & Steinberger-Wilckens, R. (2018). Systematic analysis of biomass derived fuels for fuel cells. *International Journal of Hydrogen Energy, 43*(52), 23178-23192. doi:10.1016/j.ijhydene.2018.10.161

Arghandeh, R., Amidpour, M., & Khodaei, H. (2009).

Steam network modeling and simulation in gas refinery by considering pinch technology. Paper presented at the Conference Proceedings - IEEE SOUTHEASTCON.

Bezaatpour, M., Rostamzadeh, H., Bezaatpour, J., & Ebadollahi, M. J. P. T. (2021). Magnetic-induced nanoparticles and rotary tubes for energetic and exergetic performance improvement of compact heat exchangers. *377*, 396-414.

Caliandro, P., Tock, L., Ensinas, A. V., & Marechal, F. (2014). Thermo-economic optimization of a Solid Oxide Fuel Cell - Gas turbine system fuelled with gasified lignocellulosic biomass. *Energy Conversion and Management, 85*, 764-773. doi:10.1016/j.enconman.2014.02.009

Cheddie, D. F. (2011). Thermo-economic optimization of an indirectly coupled solid oxide fuel cell/gas turbine hybrid power plant. *International Journal of Hydrogen Energy, 36*(2), 1702-1709. doi:10.1016/j.ijhydene.2010.10.089

Cheddie, D. F., & Murray, R. (2010). Thermo-economic modeling of a solid oxide fuel cell/gas turbine power plant with semi-direct coupling and anode recycling. *International Journal of Hydrogen Energy, 35*(20), 11208-11215. doi:10.1016/j.ijhydene.2010.07.082

Colpan, C. O., Dincer, I., & Hamdullahpur, F. (2007). Thermodynamic modeling of direct internal reforming solid oxide fuel cells operating with syngas. *International Journal of Hydrogen Energy, 32*(7), 787-795.

Colpan, C. O., Hamdullahpur, F., Dincer, I., & Yoo, Y. (2010). Effect of gasification agent on the performance of solid oxide fuel cell and biomass gasification systems. *International Journal of Hydrogen Energy, 35*(10), 5001-5009. doi:https://doi.org/10.1016/j.ijhydene.2009.08.083

Ebadollahi, M., Rostamzadeh, H., Seyedmatin, P., Ghaebi, H., Amidpour, M. J. T. S., & Progress, E. (2020). Thermal and exergetic performance enhancement of basic dual-loop combined cooling and power cycle driven by solar energy. *18*, 100556.

Ebrahimi, A., Ghorbani, B., & Ziabasharhagh, M. (2020). Pinch and sensitivity analyses of hydrogen liquefaction process in a hybridized system of biomass gasification plant, and cryogenic air separation cycle. *Journal of Cleaner Production, 258*, 120548. doi:https://doi.org/10.1016/j.jclepro.2020.120548

Ebrahimi, A., Ghorbani, B., Ziabasharhagh, M., & Rahimi, M. J. (2020). Biomass gasification process integration with Stirling engine, solid oxide fuel cell, and multi-effect distillation. *Journal of Thermal Analysis and Calorimetry*. doi:10.1007/s10973-020-10314-9

Ghaffarpour, Z., Mahmoudi, M., Mosaffa, A., & Farshi, L. G. (2018). Thermoeconomic assessment of a novel integrated biomass based power generation system including gas turbine cycle, solid oxide fuel cell and Rankine cycle. *Energy conversion and management, 161*, 1-12.

Ghaffarpour, Z., Mahmoudi, M., Mosaffa, A., Farshi, L. G. J. E. c., & management. (2018). Thermoeconomic assessment of a novel integrated biomass based power generation system including gas turbine cycle, solid oxide fuel cell and Rankine cycle. *161*, 1-12.

Ghazizadeh, V., Ghorbani, B., Shirmohammadi, R., Mehrpooya, M., & Hamedi, M. H. J. G. P. J. (2018). Advanced Exergoeconomic Analysis of C3MR, MFC and DMR Refrigeration Cycles in an Integrated Cryogenic Process. *6*(1), 41-71.

Ghorbani, B., Hamedi, M.-H., & Amidpour, M. J. G. P. J. (2016). Exergoeconomic evaluation of an integrated nitrogen rejection unit with LNG and NGL Co-Production processes based on the MFC and absorbtion refrigeration systems. *4*(1), 1-28.

Ghorbani, B., Roshani, H., Mehrpooya, M., Shirmohammadi, R., & Razmjoo, A. J. G. P. J. (2020). Evaluation of an Integrated Cryogenic Natural Gas Process with the Aid of Advanced Exergy and Exergoeconomic Analyses. *8*(1), 17-36.

Ghorbani, B., Shirmohammadi, R., Amidpour, M., Inzoli, F., Rocco, M. J. E. C., & Management. (2019). Design and thermoeconomic analysis of a multi-effect desalination unit equipped with a cryogenic refrigeration system. *202*, 112208.

Ghorbani, B., Shirmohammadi, R., Mehrpooya, M. J. S. E. T., & Assessments. (2020). Development of an innovative cogeneration system for fresh water and power production by renewable energy using thermal energy storage system. *37*, 100572.

Ghorbani, S., & Khoshgoftar Manesh, M. H. J. G. P. J. (2020). Conventional and Advanced Exergetic and Exergoeconomic Analysis of an IRSOFC-GT-ORC Hybrid System. *8*(1), 1-16.

Guo, Y., Yu, Z., Li, G., & Zhao, H. J. I. J. o. H. E. (2020). Performance assessment and optimization of an integrated solid oxide fuel cell-gas turbine cogeneration system.

Gustavsson, L., & Svenningsson, P. (1996). Substituting fossil fuels with biomass. *Energy Conversion and Management, 37*(6-8), 1211-1216. doi:10.1016/0196-8904(95)00322-3

Hamedi, M.-H., Shirmohammadi, R., Ghorbani, B., & Sheikhi, S. J. G. P. J. (2015). Advanced exergy evaluation of an integrated separation process with optimized refrigeration system. *3*(1), 1-10.

Hu, M., Guo, D., Ma, C., Luo, S., Chen, X., Cheng, Q., . . . Xiao, B. (2016). A novel pilot-scale production of fuel gas by allothermal biomass gasification using biomass micron fuel (BMF) as external heat source. *Clean Technologies and Environmental Policy, 18*(3), 743-751. doi:10.1007/s10098-015-1038-2

Iglesias Garcia, S., Ferreiro Garcia, R., Carbia Carril, J., & Iglesias Garcia, D. (2018). A review of thermodynamic cycles used in low temperature recovery systems over the last two years. *Renewable and Sustainable Energy Reviews, 81*, 760-767. doi:10.1016/j.rser.2017.08.049

Johnson, I., & Choate, W. T. (2008). Waste heat recovery: Technology and opportunities in U.S. industry. *Waste Heat Recovery: Technology and Opportunities in U.S. Industry*.

Jouhara, H., Khordehgah, N., Almahmoud, S., Delpech, B., Chauhan, A., & Tassou, S. A. (2018). Waste heat recovery technologies and applications. *Thermal Science and Engineering Progress, 6*, 268-289. doi:10.1016/j.tsep.2018.04.017

Kadhum, M. (2016). A review of low-grade heat recovery using organic Rankine cycle. *Int. J. Eng., TOME XIV*(1), 97-102.

Khoshgoftar Manesh, M. H., & Ameryan, M. (2016). Optimal design of a solar-hybrid cogeneration cycle using Cuckoo Search algorithm. *Applied Thermal Engineering, 102*, 1300-1313. doi:10.1016/j.applthermaleng.2016.03.156

Khoshgoftar Manesh, M. H., & Noori Shemirani, A. (2017). Simulation and Optimization of Tehran Oil Refinery Steam Network in view of Exergetic, Exergoeconomic and Environmental Analysis %J Journal of Oil, Gas and Petrochemical Technology. *4*(Number 1), 55-68. doi:10.22034/jogpt.2017.58058

Klein, S., & Nellis, G. J. f.-C. s. (2012). Mastering EES.

Kolahi, M.-R., Nemati, A., & Yari, M. J. G. (2018). Performance optimization and improvement of a flash-binary geothermal power plant using zeotropic mixtures with PSO algorithm. *74*, 45-56.

Larminie, J., & Dicks, A. (2000). *Fuel Cell Systems Explained*.

Mehr, A. S., Mahmoudi, S. M. S., Yari, M., & Chitsaz, A. (2015). Thermodynamic and exergoeconomic analysis of biogas fed solid oxide fuel cell power plants emphasizing on anode and cathode recycling: A comparative study. *Energy Conversion and Management, 105*, 596-606. doi:https://doi.org/10.1016/j.enconman.2015.07.085

Meng, Q., Han, J., Kong, L., Liu, H., Zhang, T., & Yu, Z. (2017). Thermodynamic analysis of combined power generation system based on SOFC/GT and transcritical carbon dioxide cycle. *International Journal of Hydrogen Energy, 42*(7), 4673-4678. doi:10.1016/j.ijhydene.2016.09.067

Mohn, K. J. E. o. E., & Policy, E. (2020). The gravity of status quo: A review of IEA's World Energy Outlook. *9*(1).

Mohsenipour, M., Ahmadi, F., Mohammadi, A., Ebadollahi, M., & Amidpour, M. (2019). Investigation of a Geothermal-Based CCHP System from Energetic, Water Usage and CO2 Emission Viewpoints %J Gas Processing Journal. *7*(1), 41-52. doi:10.22108/gpj.2019.118131.1058

Moradi, M., Ghorbani, B., Shirmohammadi, R., Mehrpooya, M., Hamedi, M.-H. J. S. E. T., & Assessments. (2019). Developing of an integrated hybrid power generation system combined with a multi-effect desalination unit. *32*, 71-82.

Niasar, M. S., Ghorbani, B., Amidpour, M., & Hayati, R. J. E. (2019). Developing a hybrid integrated structure of natural gas conversion to liquid fuels, absorption refrigeration cycle and multi effect desalination (exergy and economic analysis). *189*, 116162.

Pirmohamadi, A., Ghaebi, H., Ziapour, B. M., & Ebadollahi, M. J. E. R. (2021). Exergoeconomic Analysis of a Novel Hybrid System by Integrating the Kalina and Heat Pump Cycles with a Nitrogen Closed Brayton System. *7*, 546-564.

Radenahmad, N., Azad, A. T., Saghir, M., Taweekun, J., Bakar, M. S. A., Reza, M. S., & Azad, A. K. (2020). A review on biomass derived syngas for SOFC based combined heat and power application. *Renewable and Sustainable Energy Reviews, 119*. doi:10.1016/j.rser.2019.109560

Ranjbar, S. F., Nemati, A., & Kolahi, M. R. (2018). Thermodynamic Analysis and Improvement of a Flash/ORC Geothermal Plant Using ZeotropicMixtures as Working Fluids in ORC.

Rostamzadeh, H., Ebadollahi, M., Ghaebi, H., Shokri, A. J. E. c., & management. (2019). Comparative study of two novel micro-CCHP systems based on organic Rankine cycle and Kalina cycle. *183*, 210-229.

Shariati Niasar, M., Amidpour, M., Ghorbani, B., Rahimi, M.-J., Mehrpooya, M., & Hamedi, M.-H. J. G. P. J. (2017). Superstructure of cogeneration of power, heating, cooling and liquid fuels using gasification of feedstock with primary material of coal for employing in LNG process. *5*(1), 1-23.

SHEIKHI, S., GHORBANI, B., SHIRMOHAMMADI, A., & HAMEDI, M. H. J. G. P. (2014). THERMODYNAMIC AND ECONOMIC OPTIMIZATION OF A REFRIGERATION CYCLE FOR SEPARATION UNITS IN THE PETROCHEMICAL PLANTS USING PINCH TECHNOLOGY AND EXERGY SYNTHESES ANALYSIS. *2*(2), -.

Smith, R. (2005). *Chemical process: design and integration*: John Wiley & Sons.

Srinivas, T., Gupta, A., & Reddy, B. (2009). Thermodynamic equilibrium model and exergy analysis of a biomass gasifier. *Journal of Energy Resources Technology, 131*(3), 031801.

Sun, L., Doyle, S., & Smith, R. (2015). Heat recovery and power targeting in utility systems. *Energy, 84*, 196-206.

Sun, L., Smith, R. J. I., & Research, E. C. (2015). Performance modeling of new and existing steam turbines. *54*(6), 1908-1915.

Tafazoli, M., Shakeri, M., Baniassadi, M., & Babaei, A. (2017). An investigation on effect of backbone geometric anisotropy on the performance of infiltrated SOFC electrodes. *Energy Equip Syst, 5*(3), 251-264.

Taheri, M., Mosaffa, A., & Farshi, L. G. (2017). Energy, exergy and economic assessments of a novel integrated biomass based multigeneration energy system with hydrogen production and LNG regasification cycle. *Energy, 125*, 162-177.

Taheri, M., Mosaffa, A., & Farshi, L. G. J. E. (2017). Energy, exergy and economic assessments of a novel integrated biomass based multigeneration energy system with hydrogen production and LNG regasification cycle. *125*, 162-177.

Varbanov, P. S., Doyle, S., & Smith, R. (2004). Modelling and optimization of utility systems. *Chemical Engineering Research and Design, 82*(5), 561-578. doi:10.1205/026387604323142603

Wang, H. T., Wang, H., & Zhang, Z. M. (2012). Optimization of Low-Temperature Exhaust Gas Waste Heat Fueled Organic Rankine Cycle. *Journal of Iron and Steel Research International, 19*(6), 30-36. doi:10.1016/S1006-706X(12)60123-X

Zheng, R., Zhang, Y., Yu, X., He, Z., Dong, S., Li, B., . . . Lv, M. (2017). Experimental Research and Feasibility Analysis of Low-Temperature Power Generation Systems Used in Petrochemical Industry. *Journal of Energy Engineering, 143*(3). doi:10.1061/(ASCE)EY.1943-7897.0000412